



Chirped polarization volume grating for wide FOV and high-efficiency waveguide-based AR displays

Kun Yin SID Student Member | Hung-Yuan Lin SID Student Member |
Shin-Tson Wu SID Fellow

College of Optics and Photonics,
University of Central Florida, Orlando,
Florida

Correspondence

Shin-Tson Wu, College of Optics and Photonics, University of Central Florida, Orlando, FL, USA.
Email: swu@creol.ucf.edu

Funding information

GoerTek Electronics

Abstract

We demonstrate a reflective chirped polarization volume grating as a strong contender for wide field-of-view augmented reality display systems. By introducing gradient pitch along the beam propagation direction, the angular bandwidth extends dramatically from 18° to 54° while keeping over 80% average efficiency and 95% peak efficiency.

KEY WORDS

augmented reality, gradient pitch structure, liquid crystals, polarization volume grating

1 | INTRODUCTION

In the past few decades, augmented reality (AR) displays, such as Google Glass, Microsoft HoloLens, and Magic Leap One, have found interesting applications in areas such as education, health care, engineering, and gaming. To integrate the computer-generated (CG) images with see-through real-world environment, different types of optical combiners have been developed. For examples, the polarizing beam splitter (PBS) is used in traditional optical design, and the partial mirror and grating are widely used in waveguide design. Compared with the PBS approach, waveguide-based AR offers several attractive features, such as compact structure and lightweight. However, the limited field of view (FOV) remains a challenge.

Holographic volume grating (HVG)^{1,2} and surface relief grating (SRG)³ are commonly used as the combiners to couple the imaging light into the waveguide. The angular response of the combiner is directly related to the FOV of the AR system. For HVG, the angular bandwidth is determined by the index contrast. On the basis of dichromated gelatin (a common material for HVG), the index contrast can reach as high as 0.15; however, the dichromated gelatin is environmentally sensitive

and not suitable for commercial products. Thus, a more commonly used material for making HVG is a photopolymer having refractive index contrast^{4,5} of about 0.035, which results in a limited angular bandwidth (10°).^{6,7} By applying multiplexing methods to HVG, wide angular bandwidth is achievable for some thick HVGs. In terms of SRG, due to the large index contrast between polymer and air, SRG can achieve a larger angular bandwidth than HVG^{8,9}; and this tilted-groove structure is achieved by nanoimprinting method in mass production. Similar to HVG, SRG also has to address the trade-off between angular bandwidth, diffraction efficiency, and manufacturing cost. As a result, the FOV of the waveguide-based AR products is still limited by the combiner and total internal reflection (TIR). Compared with HVG and SRG, reflective PVG based on liquid crystal materials exhibits unique characteristics in both optical properties and fabrication, such as nearly 100% first-order diffraction efficiency, high index contrast, large diffraction angle, and simple fabrication process. Therefore, extensive efforts have been attempted to applying reflective polarization volume grating (PVG) for waveguide coupling.^{10–15}

To provide a promising solution of limited FOV in waveguide-based AR, here, we propose a reflective

chirped polarization volume grating (CPVG) with gradually changing period. By applying gradient pitch structure to PVG, a tripled angular bandwidth can be obtained. Then, we apply this new device in an AR system prototype to characterize its performance.

2 | PRINCIPLES

Figure 1A illustrates the schematic diagram of a uniform PVG. The horizontal periodicity (Λ_x) is defined as the distance by which LC directors rotate 180° along the horizontal direction, and the vertical periodicity (Λ_y) is the distance by which LC directors rotate 180° along the vertical direction. As shown in Figure 1B, by contrast to uniform PVG, the length of Λ_B for CPVG gradually increases from Λ_{B1} to Λ_{B2} , and the length of corresponding Λ_y also increases from Λ_{y1} to Λ_{y2} .

The relationship between Bragg periodicity (Λ_B), Λ_x , and Λ_y can be described as follows:

$$\frac{1}{\Lambda_x^2} + \frac{1}{\Lambda_y^2} = \frac{1}{\Lambda_B^2}. \quad (1)$$

In order to obtain a wider angular bandwidth, we induce gradually changing period along y direction as a modulation while the period along x direction is fixed. Several approaches to generate gradient pitch in CLC have been reported in previous studies.^{16,17} By adding about 1.5% UV dye into the PVG precursor, raising the curing temperature, and decreasing the power of UV curing light, we can precisely control the length of Λ_B , which is determined by the CLC structure. As reported in Hong et al.,¹⁸ the Λ_B along the helical axis is defined by

$$\frac{1}{\Lambda_B} = \frac{1}{\Lambda_{B1}} + \left(\frac{1}{\Lambda_{B2}} - \frac{1}{\Lambda_{B1}} \right) \frac{s}{t}, \quad (2)$$

where t is the total length of the helical axis and s is the coordinate along it, and the period length is gradually changing from Λ_{B1} ($s = 0$) to Λ_{B2} ($s = t$). By applying Equations 1 and 2 to the CPVG model while keeping Λ_x as a constant, we derive the variation of Λ_y along y direction in CPVG as follows:

$$\frac{1}{\Lambda_y} = \frac{1}{\Lambda_{y1}} + \left(\frac{1}{\Lambda_{y2}} - \frac{1}{\Lambda_{y1}} \right) \frac{y}{d} + o \left(\frac{(\Lambda_{y1} - \Lambda_{y2})^2}{\Lambda_{y1}^3} \right), \quad (3)$$

where Λ_{y1} and Λ_{y2} are the period lengths along y axis near the bottom surface and top surface, respectively, and o means the higher-order terms. Generally, $(\Lambda_{y1} - \Lambda_{y2})^2/\Lambda_{y1}^3$ is much smaller than 1 so that this term can be omitted safely, similar to that reported in Weng et al.¹⁹ Furthermore, the equation of the isophase line in CPVG can be expressed as follows:

$$\Phi_{\text{gradient,CPVG}} = \frac{\pi}{\Lambda_x} x + \frac{\pi}{\Lambda_{y1}} y + \left(\frac{\pi}{\Lambda_{y2}} - \frac{\pi}{\Lambda_{y1}} \right) \frac{y^2}{d}, \quad (4)$$

where Λ_x is the period length along x axis and d is the thickness of CPVG. Once the isophase line equation is derived, we can obtain the LC orientations inside the CPVG. These orientations define the dielectric constant matrix, which is the key parameter in the simulation. Compared with a uniform PVG, the gradient pitch profile

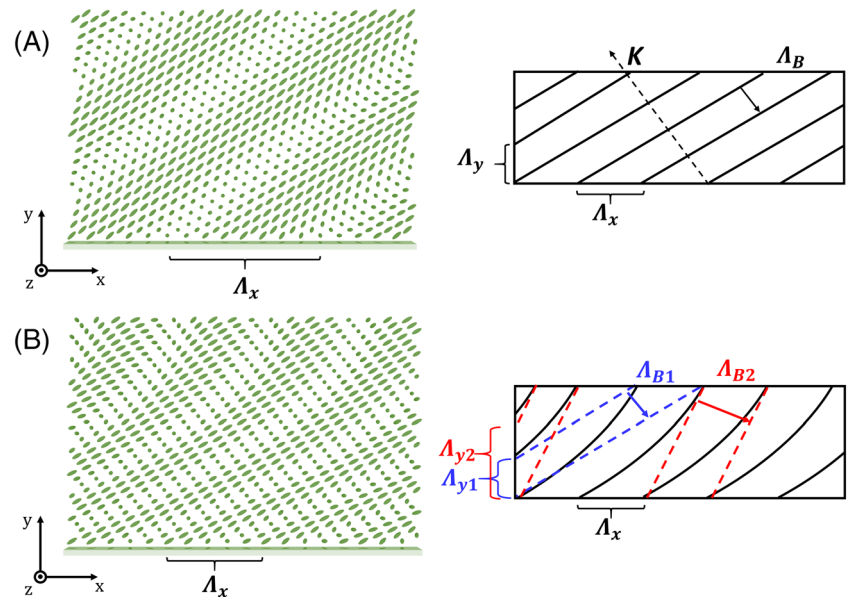


FIGURE 1 LC director profile of the uniform polarization volume grating and chirped polarization volume grating. A, The horizontal period is Λ_x , the vertical period is Λ_y , and the Bragg period is Λ_B . B, The horizontal periodicity is Λ_x , the vertical periodicities are Λ_{y1} and Λ_{y2} at the bottom and top, respectively, and the Bragg periods are Λ_{B1} and Λ_{B2} at the bottom and top, respectively

generates a series of refractive index planes with gradually changing slope.

In simulation, we assume the birefringence of a reactive mesogem RM257 is $\Delta n = 0.18$ ($n_e = 1.68$, $n_o = 1.50$) at $\lambda = 532$ nm and the thickness of the grating is 5 μm . For a uniform PVG, the period length along x and y directions is set as $\Lambda_x = 462$ nm and $\Lambda_y = 203$ nm. In terms of CPVGs, the length of Λ_{y1} and Λ_{y2} is set as 192 and 203 nm, respectively. The simulated angular response for the gradient pitch (CPVGs) and uniform pitch (PVGs) is depicted in Figure 2. The black curve in Figure 2 shows that the angular bandwidth of such a uniform PVG is around 17° (-8° to 9°) at 90% efficiency (marked with red dashed lines). In comparison with uniform PVGs, CPVGs have the angular bandwidth of 55° (from -8° to 47°) with diffraction efficiency over 90%. Our results clearly demonstrate that inducing gradient pitch significantly broadens the angular bandwidth.

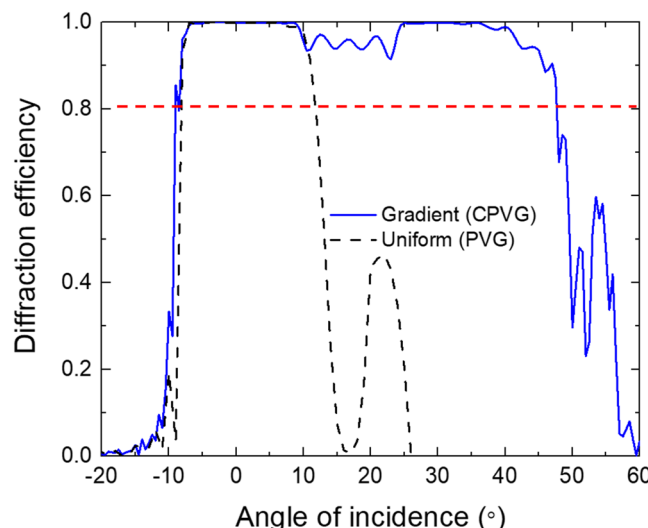


FIGURE 2 Simulated first-order diffraction efficiency: angular response at $\lambda = 532$ nm of both gradient pitch CPVGs (blue line) and uniform pitch PVG (black line)

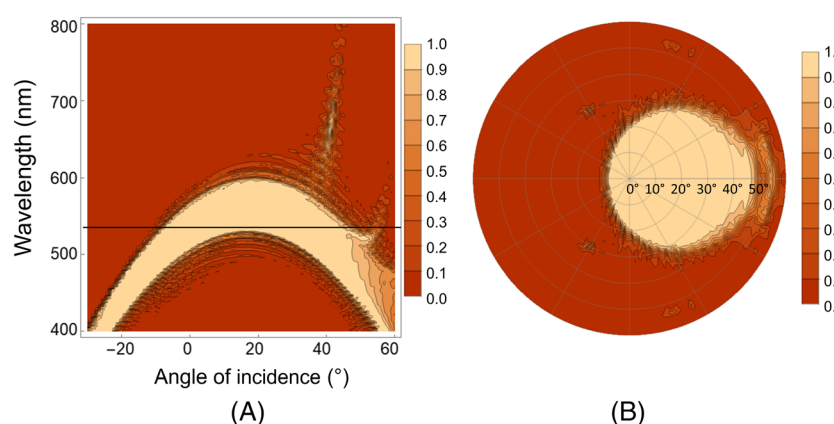


FIGURE 3 A, Simulated angular and spectral responses of the chirped polarization volume gratings. The black line shows the $\lambda = 532$ nm. B, The two-dimensional angular response of gradient pitch polarization volume grating

We also simulate the angular and spectral bandwidth of CPVGs, and results are shown in Figure 3A. Besides, we also simulate the angular response in other directions. Figure 3B shows all the angular response in the two-dimensional plane. In x direction, the angular response is asymmetric. By contrast, it is uniform and symmetric in the y direction.

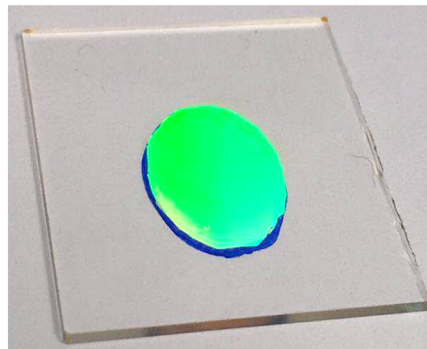
3 | RESULTS AND DISCUSSION

3.1 | Device fabrication

The fabrication procedure of reflective CPVGs is similar to that described in Yin et al¹⁴ except for different precursor and UV curing condition. The mixture consisting of 1.50-wt% UV dye (Avobenzone), 2.48-wt% chiral agent R5011 (HCCH, helical twisting power HTP $\approx 108/\mu\text{m}$), 3.00-wt% initiator Irgacure 651, and 93.02-wt% photocurable monomer RM257 (HCCH) was diluted in toluene. To generate gradient pitch, the sample was placed on a hot plate at 60°C and cured with UV light ($\lambda \approx 365$ nm, 0.3 mW/cm^2) for 40 min in nitrogen environment. Then, a CPVG working on green (532 nm) light was obtained. For red/green/blue CPVGs, they need to be fabricated separately. By controlling the chiral agent concentration, we can get different central wavelengths in the visible spectral region.

As Figure 4A shows, the photo is viewed at 50° to clearly see the diffracted green light from the CPVG sample, where the CPVG region is circled by the blue line. The text shown in Figure 4B was imaged through the sample. The distance between CPVG and camera is 1 cm, and the target is 10 cm away. The clear image seen through the CPVG region (encircled by the blue line) indicates that the scattering of the grating film is negligible. Due to the handedness selectivity, this CPVG allows more than 50% transmittance of the ambient light.

FIGURE 4 A, The chirped polarization volume grating (CPVG) sample viewed from an oblique angle with the CPVG region circled by a blue line. B, A photo taken through the CPVG sample, where the CPVG region is circled by a blue line. The distance between polarization volume grating and camera is 1 cm, and the target is 10 cm away



(A)

Using $S_2 = \frac{1}{2c} [b + \sqrt{b^2 - 4ac(T_2 - T^*)}]$, we can calculate the energy barrier against the isotropic–nematic transition. In reality, there are usually irregularities, such as superheating and supercooling. In section 3, the transition occurs simultaneously everywhere.

There are a few points worth mentioning in this section:

(B)

3.2 | Angular response

Next, we measured the angular response of CPVG using a circularly polarized green ($\lambda = 532$ nm) laser diode, and results are shown in Figure 5. The angular bandwidth is 54° (from -7° to 47°) at 80% diffraction efficiency. Compared with a uniform PVG, the angular bandwidth is three times wider. By introducing chirped structure to conventional PVGs, we can obtain a wider angular bandwidth, while keeping high efficiency and low scattering for a large FOV AR display. The angular bandwidth of CPVG is approximately two times wider than that of SRG and approximately three times wider than that of PVG and HVG. Besides, the experimental data agree with the simulation results reasonably well, although the measured diffraction efficiency is about 10% lower than the simulated one. The main reason is that the LC alignment is quite sophisticated, including horizontal subwavelength period and vertical gradient period. Any

disturbed alignment would decrease the diffraction efficiency.

4 | POTENTIAL APPLICATIONS IN AR DISPLAYS

Figure 6A illustrates the structure of a simplified AR optical system with input/output couplers and image source. When the light enters the input CPVG, it would be diffracted into the waveguide with a designed angle and then propagates following the TIR. After the output CPVG is hit, the light would be diffracted out of the waveguide into the observer's eye.

To demonstrate the feasibility of CPVG for AR displays, we fabricated two CPVGs with the same diffraction angle and working wavelength but different diffraction efficiencies. The input and output couplers were then assembled with a glass slab using optical glue (Norland Optical Adhesive 65). As shown in Figure 6B, the input and output gratings are circled in red dashed lines. First, we use a 532-nm laser diode to demonstrate that the incident light can be coupled into the waveguide through CPVG. The light from the laser diode is incident on the input area perpendicular to the glass slab. After being coupled into the waveguide by the input coupler, the light propagates inside the glass slab due to TIR. When entering the output area, the light will be diffracted out of the glass slab into the observer's eye by the output CPVG. From Figure 6B, we can clearly see the input light spot, TIR spots, output points, and the leaked light.

Next, we used a micro-organic LED as the image source to build an AR optical system. Figure 7 is a picture of our AR prototype. Here, we combine a micro-organic LED with a lens to generate collimated input image. Figure 8 shows the experimental results. We send a green "A" as the input image into the assembled AR device and then take a picture at

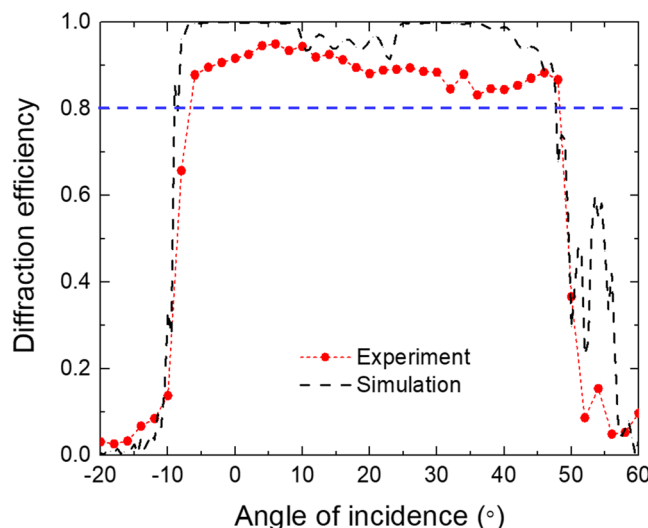


FIGURE 5 Angular behavior of optical efficiency. The black line is the simulation results, and the red dots denote the measured results of chirped polarization volume grating sample

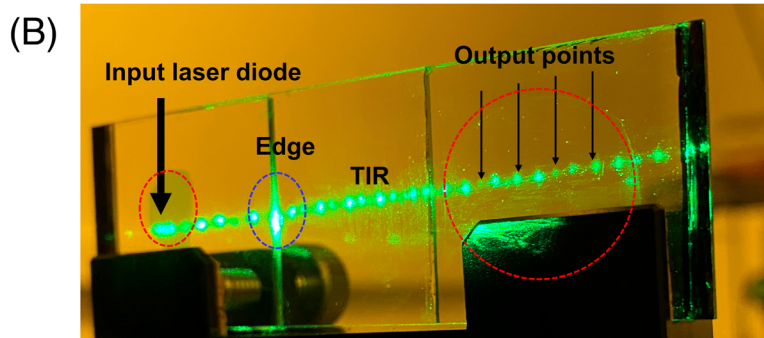
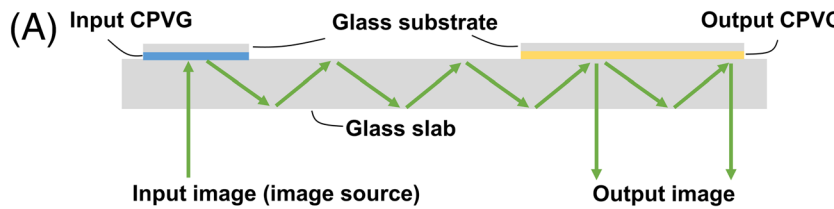


FIGURE 6 A, Top view of a simplified augmented reality module. B, Photo of an augmented reality module with a green laser diode input light

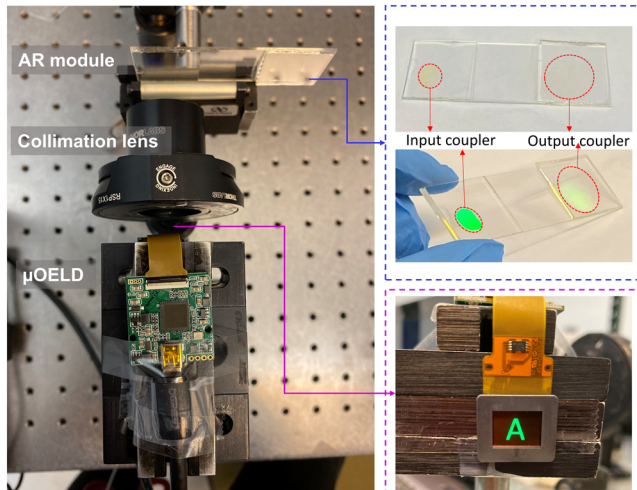


FIGURE 7 Picture of an augmented reality prototype, including a micro-organic LED panel and two chirped polarization volume gratings



FIGURE 8 Photo of the output image

output. The coupled-out image is quite uniform but a little blur. Because when the light propagates in the waveguide (glass slab), the TIR may occur at or near to the edge of the CPVG substrate. As depicted in Figure 6B, the light leakage and scattering at the edge of the glass substrate are circled by blue dashed lines. Therefore, the light is scattered by the rough surface of the glass edge. Such a rough edge is caused by our laboratory fabrication equipment and can be eliminated by better assembly method in the future. Besides, the optical glue that we used to assemble the module will also accumulate at the edge and scatter the light. In general, the results show the feasibility of our CPVG for AR systems. Although the output

image is slightly hazy and the background is not bright enough, the prototype still shows good performance.

5 | CONCLUSION

We have experimentally demonstrated CPVGs with an extra-large angular bandwidth while keeping optical efficiency over 80%. This is achieved by inducing gradient pitch along the beam propagation direction. Specifically, our CPVG possesses 54° angular bandwidth, over 80% average efficiency, and 95% peak efficiency. Next, we use this device to build an AR prototype and

demonstrate the feasibility. Due to its wide angular bandwidth, high efficiency, low scattering, high transmittance, and simple fabrication process, our CPVG would be a strong contender for see-through near-eye displays.

ACKNOWLEDGMENT

The authors are indebted to GoerTek Electronics for the financial support.

ORCID

Kun Yin  <https://orcid.org/0000-0002-5624-4915>

Shin-Tson Wu  <https://orcid.org/0000-0002-0943-0440>

REFERENCES

1. Kasai I, Tanijiri Y, Takeshi EN, Hiroaki UE. A practical see-through head mounted display using a holographic optical element. *Opt Rev.* 2001;8(4):241–244. <https://doi.org/10.1007/s10043-001-0241-z>
2. Mukawa H, Akutsu K, Matsumura I, et al. A full-color eyewear display using planar waveguides with reflection volume holograms. *J Soc Inf Display* 2009;17(3):185–193. <https://doi.org/10.1002/j.2637-496x.2009.tb00066.x>
3. Kress BC, Cummings WJ. Towards the ultimate mixed reality experience: HoloLens display architecture choices. *SID Int Symp Digest Tech Papers.* 2017;48(1):127–131. <https://doi.org/10.1002/sdtp.11586>
4. Sabel T, Zschocher M. Transition of refractive index contrast in course of grating growth. *Sci Rep.* 2013;3(1):2552. <https://doi.org/10.1038/srep02552>
5. Bruder F, Fäcke T, Hagen R, et al. Diffractive optics with high Bragg selectivity: volume holographic optical elements in Bayfol® HX photopolymer film. *Proc SPIE.* 2015;9626:96260T. <https://doi.org/10.1117/12.2191587>
6. Zhang N, Liu J, Han J, et al. Improved holographic waveguide display system. *Appl Optics.* 2015;54(12):3645–3649. <https://doi.org/10.1364/ao.54.003645>
7. Escuti MJ, Kossyrev P, Crawford GP, Fiske TG, Colegrove J, Silverstein LD. Expanded viewing-angle reflection from diffuse holographic-polymer dispersed liquid crystal films. *Appl Phys Lett.* 2000;77(26):4262–4264. <https://doi.org/10.1063/1.1335544>
8. de Jong TM, de Boer DK, Bastiaansen CW. Surface-relief and polarization gratings for solar concentrators. *Opt Express.* 2011;19(16):15127–15142. <https://doi.org/10.1364/oe.19.015127>
9. Bai B, et al. Optimization of nonbinary slanted surface-relief gratings as high-efficiency broadband couplers for light guides. *Appl Optics.* 2010;49(28):5454–5464. <https://doi.org/10.1364/ao.49.005454>
10. Kobashi J, Yoshida H, Ozaki M. Planar optics with patterned chiral liquid crystals. *Nat Photon.* 2016;10(6):389–392. <https://doi.org/10.1038/nphoton.2016.66>
11. Yin K, Lin HY, Wu ST. Chirped polarization volume grating with ultra-wide angular bandwidth and high efficiency for see-through near-eye displays. *Opt Express.* 2019;27(24):35895–35902. <https://doi.org/10.1364/oe.27.035895>
12. Lee YH, Yin K, Wu ST. Reflective polarization volume gratings for high efficiency waveguide coupling augmented reality displays. *Opt Express.* 2017;25(22):27008–27014. <https://doi.org/10.1364/oe.25.027008>
13. Yin K, Lee YH, He Z, Wu ST. Stretchable, flexible, and adherable polarization volume grating film for waveguide-based augmented reality displays. *J Soc Inf Display* 2019;27(4):232–237. <https://doi.org/10.1002/jsid.770>
14. Yin K, Lee YH, He Z, Wu ST. Stretchable, flexible, rollable, and adherable polarization volume grating film. *Opt Express.* 2019;27(4):5814–5823. <https://doi.org/10.1364/oe.27.005814>
15. Lee YH, Tan G, Yin K, Zhan T, Wu ST. Compact see-through near-eye display with depth adaption. *J Soc Inf Display* 2018;26(2):64–70. <https://doi.org/10.1002/jsid.635>
16. Broer DJ, Lub J, Mol GN. Wide-band reflective polarizers from cholesteric polymer networks with a pitch gradient. *Nature.* 1995;378(6556):467–469. <https://doi.org/10.1038/378467a0>
17. Katsis D, Kim DU, Chen HP, Rothberg LJ, Chen SH, Tsutsui T. Circularly polarized photoluminescence from gradient-pitch chiral-nematic films. *Chem Mater.* 2001;13(2):643–647. <https://doi.org/10.1021/cm0008011>
18. Hong Q, Wu TX, Wu ST. Optical wave propagation in a cholesteric liquid crystal using the finite element method. *Liq Cryst.* 2003;30(3):367–375. <https://doi.org/10.1080/0267829031000083777>
19. Weng Y, Xu D, Zhang Y, Li X, Wu ST. Polarization volume grating with high efficiency and large diffraction angle. *Opt Express.* 2016;24(16):17746–17759. <https://doi.org/10.1364/oe.24.017746>

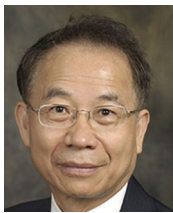
AUTHOR BIOGRAPHIES



Kun Yin received a BS degree in Opto-Electronics from Tianjin University of China in 2016 and is currently working toward a PhD degree from the College of Optics and Photonics, University of Central Florida, Orlando. Her current research interests include novel optical components based on liquid crystal materials and optical system design for augmented reality and virtual reality displays.



Hung-Yuan Lin Hung received his MS degree in Photonics from the National Sun Yat-sen University of Taiwan in 2018 and used to be a visiting scholar from the College of Optics and Photonics, University of Central Florida, Orlando. His research interests focus on the smart window and augmented reality displays and liquid crystal-based devices.



Shin-Tson Wu is Pegasus professor at the College of Optics and Photonics, University of Central Florida. He is among the first six inductees of the Florida Inventors Hall of Fame (2014) and a Charter Fellow of the National Academy of Inventors (2012). He is a fellow of the IEEE, OSA, SID, and SPIE and an honorary professor at Nanjing University (2013) and at National Chiao Tung University (2017). He is the recipient of 2014 OSA Esther Hoffman Beller Medal, 2011 SID Slottow-Owaki Prize, 2010

OSA Joseph Fraunhofer Award, 2008 SPIE G. G. Stokes Award, and 2008 SID Jan Rajchman Prize. Presently, he is serving as SID honors and awards committee chair.

How to cite this article: Yin K, Lin H-Y, Wu S-T. Chirped polarization volume grating for wide FOV and high-efficiency waveguide-based AR displays. *J Soc Inf Display*. 2020;28:368–374. <https://doi.org/10.1002/jsid.893>